

Prediction of System Evolution by Learning Machine

Hong Zhao

Department of Physics, Xiamen University,

Xiamen 361005, China

E-mail: zhaoh@xmu.edu.cn

The orthodox approach for understanding a dynamical system is to establish its equation of motion, by which one can unveil its dynamical behavior at a given system parameter set, and reveal how the dynamic behavior evolves as the system parameters change. Here we show that this task can be fulfilled with a learning machine in a model-free way. We find that, based only on a segmental time series of a state variable recorded at present stage, the dynamics exhibited by the learning machine at different training stages can be mapped to the dynamics of the target system along a particular path in its parameter space following an appropriate training strategy that monotonously decreases the cost. This path is important, because along which the primary dynamical properties of the target system will emerge subsequently, in the simple-to-complex order, matching closely to the evolution of a natural system. A theoretical framework is proposed to explain the underlying mechanism. This revealed function of the learning machine opens up a novel way to probe the global dynamical properties of a black-box system without the equation of motion established artificially, and as such it might have huge potential applications. As an application example, this method is applied to infer what dynamical stages a variable star has experienced and how it will evolve in future by using the light curve observed presently.

Introduction

Dynamical systems are the basic objects of scientific research. They have applications in a wide variety of fields ranging from physics, biology, chemistry, engineering, economics, and medicine to beyond. In general, the motion of a dynamical system can be described by $\mathbf{x}(t) = f^t(\mathbf{x}(0), \mathcal{A})$, where $\mathbf{x} \in R^d$ is a d -dimensional vector variable, t is the time, f^t is the evolution operator, and \mathcal{A} is the parameter set. By investigating the entire parameter space one can grasp the global dynamical behavior of the system. The inverse-problem approach, one of the most important mathematical tools in science, is aimed to modelling a system by finding its parameters from a data set of observations (1-2). The equation of motion of the system is pre-estimated based on physical considerations. However, to accurately model a real-world system is an especially difficult problem – it needs accurate prior knowledge about the system. Without the model, if a certain variable of the system, $x(t)$, is measured over a period of time, there are some model-free approaches that can be applied to predict the future evolution of this variable, such as the time series reconstruction methods (3-4),

empiricism-based methods (5), deep belief network (6), long short-term memory network (7), and reservoir computing (8–10), etc.. This kind of prediction is done, however, for the *evolution of variable states* under a fixed system parameter set \mathcal{A} . A more challenging task is to predict the *system evolution* in a model-free way under the same premise, i.e., to infer the dynamical properties the system may exhibit in its entire parameter space, by using only time series of certain variables measured at present parameter set \mathcal{A} .

Here we report that by employing the learning machine, this task can be fulfilled. We find that under an appropriate training strategy, the dynamics of the learning machine observed at different training stages may reproduce the dynamics of the target system along a special path in its parameter space. This path is particularly important since along which, the overall dynamical behavior of the target system, from simple to complex, is reproduced qualitatively. We then employ a simplified undetermined-parameter model to explain why the learning machine can reveal the dynamics of the target system out of the parameter region where the training data are collected. It is found that the data can impose restrictions on the global dynamics of the learning machine, and cause its parameter space collapsing onto a subspace in which the learning machine appears to be equivalent to the target system. The learning machine reproduces the dynamics from simple to complex as a consequence of the constraint of the cost function applied. The Lorentz system, one of the best-known and the most complex models in nonlinear dynamics study, is adopted as the illustration example.

The simple-to-complex path is inherently consistent with the usual evolution law of natural systems. Taking the current stage as a reference point, the learning machine can not only reproduce the evolution history of a target system, but also predict how it will evolve in future. As an example, we apply the learning machine to study the system evolution of variable stars based on the observed light curves. Observations indicate that more than 30% of stars exhibit luminosity changes; variable stars are among them and have been used as the standard candles to measure the cosmic distance, but their evolutionary paths have not been fully understood (11-15) yet. The time scale of human observation records is extremely short compared with the cosmological time scale, and thus it is impossible to explore the evolution process of the specific variable stars by direct observation. In the duration of records, the stars correspond to a fixed-parameter system. The learning-machine method discussed in this work provides a possible tool in the variable star case to infer their evolutionary path and to improve their classification.

Results

Learning machine and training strategies.

The dynamics of our three-layer self-evolution learning machine is described by a time-delayed map

$$\Phi(n+1) = \Phi(n) + \tau \sum_i^N u_i f(\beta_i \sum_{j=1}^{M-1} v_{ij} \Phi(n-j) - b_i), \quad (1)$$

where M and N are the number of input and hidden layer neurons, respectively, τ is the

time interval between two sequential records of the target system's time series, and f is the neuron transfer function. In this paper, we fix the neuron transfer function to be $f(h) = \exp(-h^2)$. Besides M and N , the learning machine contains four types of parameters, each is bounded in an interval, i.e., $|u_i| \leq c_u, |\beta_i| \leq c_\beta, |v_{ij}| \leq c_v, |b_i| \leq c_b$. (We call c_u, c_β, c_v, c_b training control parameters.) The parameters are randomly initialized in their value ranges. Note that our learning machine can be considered as a simplified variation of reservoir computers. Nevertheless, all of the parameters in our model are adjustable.

Let $x(j), j = 1, \dots, P$ be a segmental time series of a variable x recorded in the time interval τ . We use it to construct $P-M$ training samples, with $\{\Phi(n-j) = x(n-j), j = M-1, \dots, 0\}$ being the input of the n th sample and $x(n+1)$ the expected output. We define the cost function as

$$\lambda = \left(\frac{1}{P-M} \sum_{n=M}^{P-M} (x(n+1) - \Phi(n+1))^2 \right)^{1/2} \quad (2)$$

and apply a simple Monte Carlo algorithm to train the learning machine: Randomly mutating a parameter in its value range and accepting this variation if it does not increase λ . We note that this algorithm is practical for applications. However, we would like not to discuss this issue because the purpose of this paper is to demonstrate the feasibility for predicting the system evolution by the learning machine.

Our first goal is to find a set of optimal values of the control parameters c_u, c_β, c_v, c_b for the fixed M and N . With such an optimal set, when λ reaches a critical value λ_c , the learning machine's output can best simulate the subsequent output of x . By "best simulate", we mean it results in not only an accurate, quantitative prediction, but also a qualitative imitation with high statistical similarity to the future evolution of the output. What is achieved at this stage is the variable evolution prediction.

We then, with the optimal control parameters, train the learning machine with reinitialized parameters again. After a fixed amount of Monte Carlo operations, the training is suspended with a new λ reached. Then, let the learning machine self-evolve for a long enough time to skip the transient process, a set of the delay coordinates, $\Phi(t_c - T)$, is recorded hereafter, where t_c is the time that $\Phi(t)$ crosses the section of $\Phi(t) = c$ from above, and T is a delayed time. In this way, we obtain the bifurcation diagram of the learning machine along the axis of $1/\lambda$, which represents the global dynamics of the learning machine in the training process.

An illustration example

The Lorentz system is given by $dx/dt = -\sigma(x - y)$, $dy/dt = -xz + Rx - y$, and $dz/dt = xy - Bz$. Figure 1(a) shows the bifurcation diagram of the system along the parameter B with other two parameters fixed at $(\sigma, R) = (10, 28)$. Here the vertical axis represents $x(t_c - 0.1)$, which is the delayed coordinate of the section point t_c that the x variable crosses the section of $x=5$. It can be seen that the global dynamics of the Lorentz system is very complicated; there are many stages with coexisting attractor branches.

In Fig. 1(b), the period-doubling bifurcation route to chaos is shown, which is ubiquitous in nonlinear dynamical systems. In Fig. 1(c) several representative trajectories along the bifurcation diagram are plotted. The trajectories are represented by $[x(t)-x(t-0.1)]$ here.

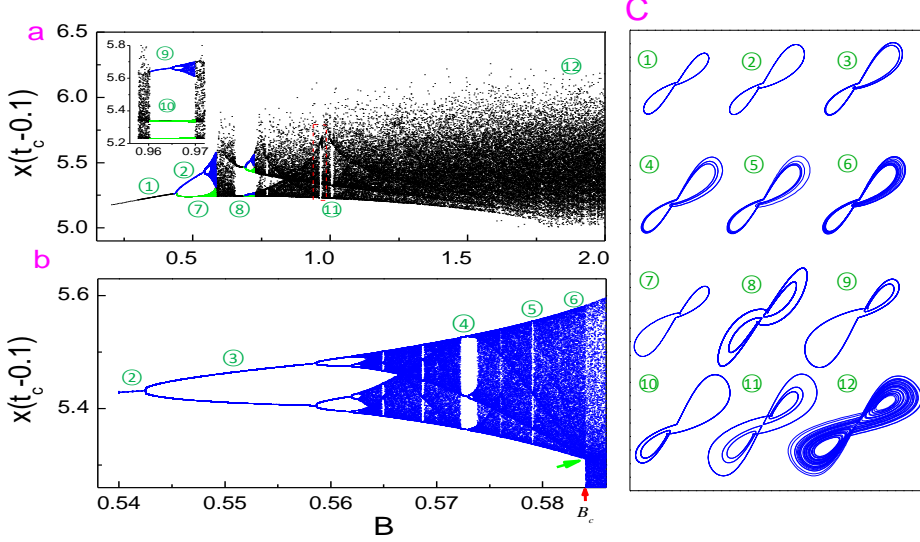


Figure 1: The global dynamics of the Lorenz system. (a), The bifurcation diagram along parameter B . The pieces colored in blue and green are coexisting attractor branches at the same parameter region. The inset is a zoom-in of the area marked by the red rectangle. (b), The zoom-in of the blue piece panel a for $B \in (0.54, 0.6)$. The critical point $B_c \approx 0.5845$ is indicated by a red arrow. At this point the two pieces (blue and green for $B < B_c$ shown in panel (a) of coexisting-attractor branches merge with each other. Note that several 'dark lines' intersect at a point on the line of $B = B_c$ (blue arrow). (c), Typical trajectories along the bifurcation diagram represented by delayed coordinates $x(t) - x(t-0.1)$ with the same coordinate scale. The corresponding parameter values of B for these trajectories are indicated by the positions of their serial numbers in panel a and b.

We consider two training sets at $B = 0.555$ and $B = 1.9$, respectively. The other two parameters are fixed at $(\sigma, R) = (10, 28)$. Each set involves a time series segment of x variable of length $t=30$ recorded with the interval of $\Delta t=0.01$. In the bifurcation diagram, the first one is constructed at the position marked by digit 3 in Fig. 1(b), which appears as a period-2 limit cycle. The second is a chaotic trajectory marked by digits 12 in Fig. 1a. The delayed coordinate representations of these two training sets are shown in Fig. 1(c), while their time series are shown in Fig. 2. We use them to train respectively two learning machines with $N=3000$ and $M=50$.

By finding the corresponding optimal control parameters (see SM-Fig. 1), we achieve the best reproduction (see Fig. 2(a) and 2(b)) of the two training sets successfully. The bifurcation diagram (Fig. 3(a)) of the learning machine trained by the limit cycle reproduces Fig. 1(b) in the parameter range of $B \in (0.45, B_c)$ precisely, even the dark line structure. More strikingly, the trajectories along the two bifurcation diagrams have the identical topology, in spite of the different amplitudes (compare Fig. 1(c) and Fig. 3(d)). Therefore, the learning machine proves to be equivalent to the target system in this case. In particular, at $\lambda = \lambda_c$ it is identical to the target system with the assigned parameter $B = 0.555$, and for $\lambda > \lambda_c$ and $\lambda < \lambda_c$ it reproduces/predicts the dynamics

of the target system with $B < 0.555$ and $B > 0.555$.

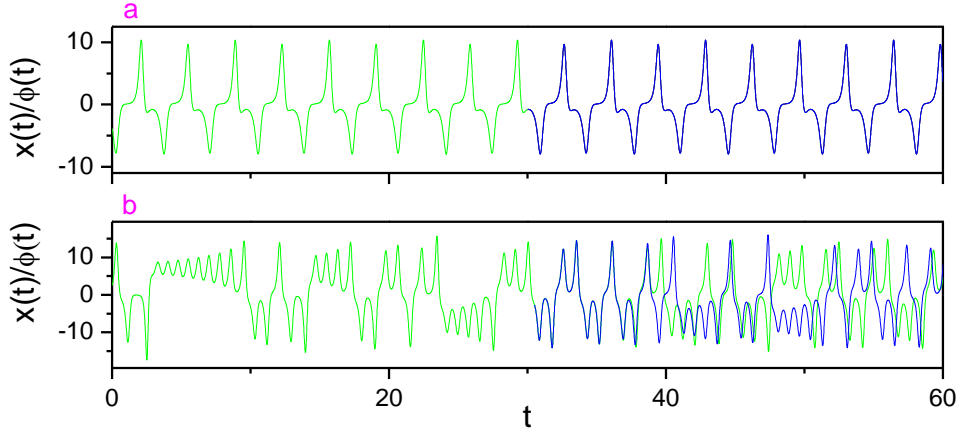


Figure 2: Variable evolution prediction for the Lorenz system. (a) and (b) show the sampled (green) and the mimicked trajectory (blue) at $B=0.555$ and 1.9 , respectively. The segmental time series in the time interval $t \in (0,30)$ are adopted to train two learning machines, respectively.

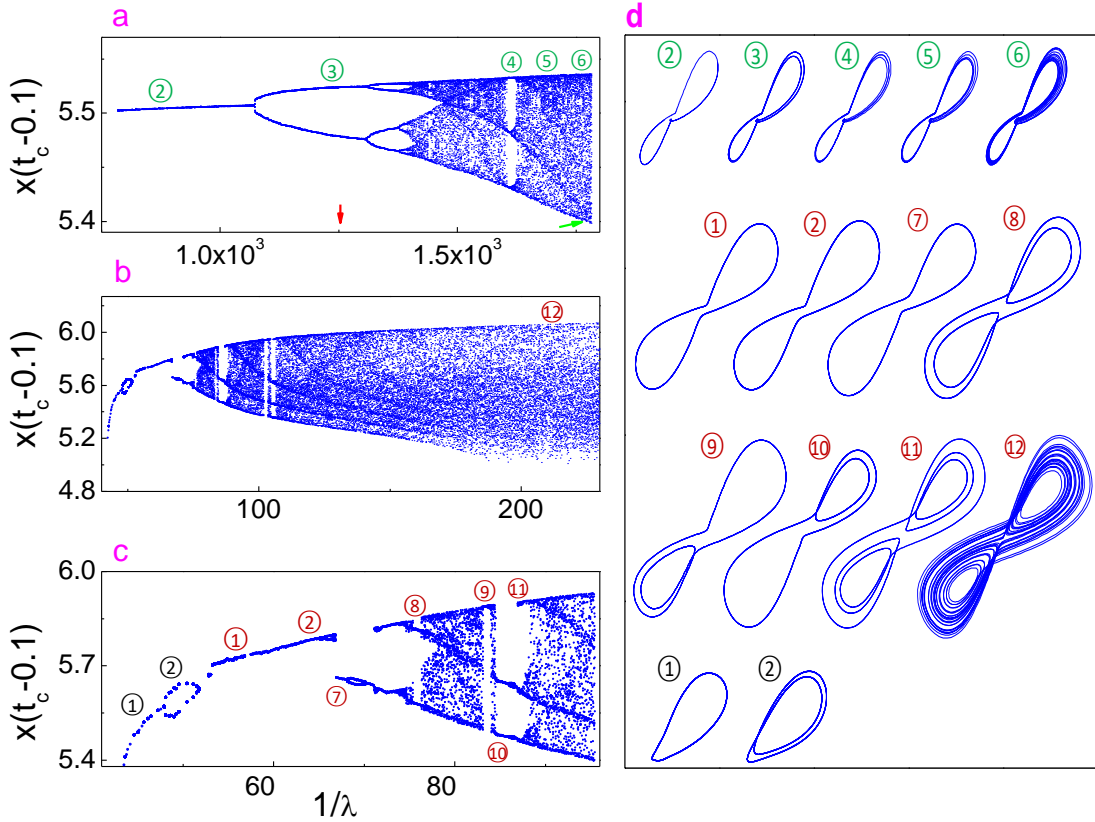


Figure 3: The global dynamics of the learning machine. (a) and (b) give the bifurcation diagrams of the learning machines trained by the sample shown in Fig. 2(a) and 2(b), respectively. (c) is a zoom-in of (a) part of (b). (d) shows representative trajectories whose positions in the bifurcation diagram are marked by the corresponding serial numbers. The bifurcation diagram in panel a reflects faithfully that of the target system shown in Fig 1(b) for $B \in (0.45, B_c)$. All period windows in Fig. 1b can be identified in Fig. 2(a), correspondingly. The trajectories of the learning machine and the

target system have the same topology at each stage, even the ‘dark lines’ have the similar structure. Although Fig. 3(b) does not look like Fig 1(a) very much, Fig. 3(d) indicates that all the primary limit cycles are reproduced by the learning machine, even when they are far from the point in the bifurcation diagram where the training sample is produced. Particularly, those limit cycles marked by black digit 1 and 2, which do not appear in the bifurcation diagram Fig.1(a) but can be found in the corner of the parameter region around $B=0.05$, appear in the bifurcation diagram of the learning machine.

We have checked that the training sample produced at any point in the interval of $0.45 < B < B_c$ leads to qualitatively the same bifurcation diagram (see SM-Fig.2). In more detail, no matter how close it is to the point B_c , the resulted bifurcation diagram recovers that of the target system only before $B=B_c$. The recovery fails hereafter, manifested as a quick divergence or a sudden change in the amplitude of its output (the output no longer maintains a clear similarity with that of the target system). Note that $B=B_c$ is a crisis point, at which the two coexisting-attractor branches collide [Fig.1(a)]. Therefore, the prediction ability of the learning machine could be limited by certain intrinsic properties of the target system as the crisis does that can abruptly increase the complexity. This restriction, on the other hand, can be interpreted as that the learning machine can predict the crisis. This property may have application importance, considering that the earthquake, atrial fibrillation, epilepsy, etc., are crises.

The bifurcation diagram of the learning machine trained with the sample at $B = 1.9$ has a certain degree of deformation in the early region compared with that of the target system (see Fig. 3(b) and 3(c), and make a comparison to Fig.1(a)). However, by examining the output time series at different stages, we find that the primary limit cycles that have appeared in period windows along the bifurcation diagram of the target system are reproduced (see Fig.1(c) and Fig. 3(d)). These windows distributed in the region of $B < 1$, far from the parameter value of $B = 1.9$ at which the training sample is collected. Note that an extra segment in the beginning of the bifurcation diagram shows up and two trajectories, marked by black digit 1 and 2 on this segment, are also shown in Fig. 3(d). Interestingly, by carefully checking the target system, we do find that there exist these solutions around $B=0.05$. On the other hand, the learning machine also loses certain information of the target system. The primary limit cycles remain but, taking the two period-1 limit cycles, marked by 2 and 7, for example, the subsequent period-doubling cascade loses. In addition, the coexisting-attractor branches appear simultaneously in the bifurcation diagram of the target system may appear discontinuously along the axis of $1/\lambda$ (see Fig. 3(c)), implying the breaking of the symmetry of the target system.

In clear contrast, for a target system with simple dynamics, for example, a harmonic oscillator, we can achieve the mimic of its dynamics by a learning machine. In this case, however, no complicated motion shows up (see SM-Fig. 3) as the cost parameter λ is changed.

The mechanism

In the parameter space of a target system, there are various paths connecting to a

specific point, and the bifurcation diagram along different paths may be significantly different (see SM- Fig.4). It seems very unlikely that the training data collected at this point are sufficient to reproduce the dynamics along a given path, in particular the one that follows the evolution law from simple to complex. To figure out the underlying mechanism for this magic function of the learning machine, we consider an undetermined-parameter model: Fixing the last two equations of the Lorenz system and rewriting the first one as $d\tilde{x}/dt = c_1\tilde{x}\tilde{y} + c_2\tilde{x}\tilde{z} + c_3\tilde{y}\tilde{z} + c_4\tilde{x} + c_5\tilde{y} + c_6\tilde{z}$. We take a segmental trajectory $\{x(n-I), y(n-I), z(n-I), n=0, \dots, P\}$ of the original Lorenz system at $B=0.555$ to train the model. The Monte Carlo operation is applied to decrease the cost function $\lambda = (\frac{1}{P} \sum_{n=1}^P (x(n) - \tilde{x}(n))^2 + (y(n) - \tilde{y}(n))^2 + (z(n) - \tilde{z}(n))^2)^{1/2}$. In Fig. 4(a), it can be seen that as λ decreases, c_1, c_2, c_3 , and c_6 converge to zero from their randomly initialized values after a short transient period while the parameters c_4 and c_5 will evolve gradually to $c_4=-c_5=10$. Namely, the training will first lead the learning machine to approach to the target system at different parameters, and then converge to the target system at the parameter set with which the training data are collected. It suggests that the training data can impose strict intrinsic restrictions (such as topology) on the undetermined-parameter model, and causes it collapse onto the target system before the present state is approached.

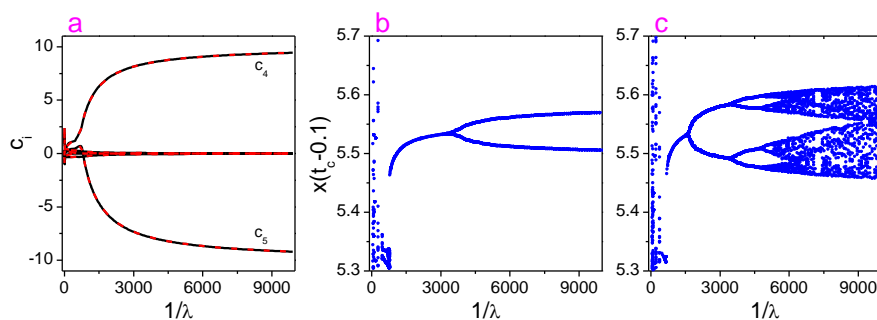


Figure 4: An illustration of the reproduction mechanism. (a), The undetermined-parameter models converge to the target system (with $c_1=c_2=c_3=c_6=0$) in a very short time, and then evolves towards the target parameter point ($c_4=-c_5=10$) where the training data is collected. The solid and dashed lines represent the parameter change for the undetermined-parameter models without and with its first equation of motion being slightly changed. It has been checked that different initialization of c_i gives qualitatively the same result. (b) and (c), The bifurcation diagrams in the training process for the model and the changed model, respectively. The former reproduces only the ‘past’ while the latter reproduces not only the ‘past’ but also the ‘future’.

Fig. 4(b) shows that the bifurcation diagram of the undetermined-parameter model as a function of λ . The model evolves from a period-1 limit cycle to the training sample of period-2 limit cycle. It can be checked that this bifurcation diagram corresponds to the part before $B=0.555$ in Fig. 1(a). Therefore, with this setting the training process drives the parameter set converges exactly to the training parameter set, leading the bifurcation diagram to end exactly at the period-2 limit cycle of the training set. The

cascade bifurcation dynamics afterwards have not been explored, i.e., the reproduce is achieved only for $B < 0.555$.

We then make a slight change to the undetermined-parameter model, say to change the first equation of motion to be $dx/dt = -\sigma(x - y) + 0.001\tilde{z}$ by adding the perturbation given by the last term, so to prohibit an exact convergence to the target system. In this case, Fig. 4(c) shows that the global convergent behavior is identical to that of Fig. 4(a). Nevertheless, the subsequent cascade bifurcations take place and the dynamics for $B > 0.555$ is reproduced qualitatively (Fig. 4(d)). Therefore, a slightly mismatched undetermined-parameter model is helpful for exploring the global dynamics beyond the present stage.

The undetermined-parameter model is a simplified version of the learning machine. Based on above illustrations, it can be understood why the learning machine first approaches the target system with lower-order complexity and why it can explore the global dynamics of the target system along a special path in the parameter space. In the initial stage of training, the trajectories of the learning machine still keep distant from the training trajectory. With such an uncertainty, the training trajectory provides just a target of region of convergence, and its finer structure does not play a role yet. Based on the dynamical system theory, in a nonlinear system, an attractor with lower-order complexity usually has bigger ability of attraction, leading to a faster convergence of nearby trajectories to the attractor. Thus, at this stage, the parameter set at which the attractor leading to the faster convergence can be approached more easily by our training process, since it results in a faster decreasing of the cost function. Which parameter set is approached first actually is of course also determined by the training set. As the training progresses further, the finer structure begins to play a more and more important role, forcing the learning machine to evolve towards the parameter set that the training data are collected. Furthermore, if the learning machine is close enough to the target system, but not equivalent to it strictly, the path may pass the present parameter set and explore more global dynamic behavior. The training process thus induces a path in the parameter space along which the system evolves from simple to complex.

The learning machine has a huge number of undetermined parameters, and its properties can be controlled by the training control parameters. There thus is a huge freedom to allow it to collapse onto a counterpart of the target system. Meanwhile, due to the difference in architecture, the learning machine may not be equivalent exactly to the target system, and this makes it possible for the learning machine to explore the dynamical properties of the target system beyond the parameters with which the training data are produced. How close the learning machine is to the target system can be controlled by the learning machine size N , and the larger the N , the closer the two systems. As a consequence, the learning machine can be applied as a general template model to qualitatively reproduce the system evolution. The learning machine is in fact significantly superior to the undetermined-parameter model. For the latter, a prior knowledge of the target system must be used, and even worse is that this model is found having a bad convergent property if being extended to involve more undetermined parameters, e.g., rewriting other two equations also as the undetermined forms in our

example Lorentz model. Meanwhile, it is worth noting that our scheme is only one feasible way for model-freely probing the global dynamics of a black-box system. A lot of basic theoretical and technical issues remain to be resolved, in particular how to decide to terminate the training process to guarantee that the dynamics emerging from the learning machine hereafter represents that of the target system.

Application to variable stars

There are various types of variable stars. Some of them show simple single or multi pulsation frequencies. Certain variable stars are found to pulsate with two principal frequencies nearly in the golden ratio while many others may show the Blazhko effect. The second pulsation frequency to the fundamental frequency of the Golden stars is about $f_0/f \sim 0.618$ [11]. The Blazhko effect refers to the phenomenon that the light curve has a periodic amplitude and/or phase modulation (12). The modulation period may be single-periodic, multi-periodic or irregular (13-14). Certain Blazhko stars pulsate intermittently with double period of the fundamental one (15). Our purpose here is to clarify their classification along the evolutionary route.

The Kepler space telescope provides the best light curves of variable stars so far (16-20). There are 16 measurement modules in the database. Due to instrument adjustment and other reasons, there are big biases between different module data. In order to avoid the biases, we only use the data in one module as a training sample to avoid possible misleading due to preprocessing. As such, the length of our training data is within 3 months. Figure 5(a) and 5(c) show the light curve samples for two typical variable stars, KPL7198959 and KPL5520878, respectively. The former is a Blazhko-effect star with period doubling characteristic and the latter represents a typical class of non-Blazhko-effect variable stars.

In Fig. 5(a), the predicted light curve under the corresponding optimal control parameters is also shown. We see that the learning machine gives a good prediction of the present light curve; i.e., it provides not only a perfect period recovery but also a good amplitude prediction for a long period of time. Particularly, the period-doubling characteristics emerges in an intermittent manner, consistent with the observed phenomenon.

Based on the bifurcation diagram (Fig.5(b)) together with pulsation patterns (Fig. 5(e)), it can be inferred that at its early time, KPL7198959 performed a simple single-period pulsation. Later it evolved into a Blazhko-effect stage via a Hopf bifurcation. After the bifurcation, this variable star began to pulsate with the Blazhko effect but without the period-doubling characteristics. Then it came to the current stage, a Blazhko-effect stage with the period-doubling characteristics. In future, the pulsation may develop into one of multi-cycle or even an irregularly modulated Blazhko-effect stage, as the pattern marked by digit 4 shows. Other Blazhko-effect stars have the similar bifurcation diagram, but the period-doubling characteristics may not be predicted for certain (see SM-Fig. 5).

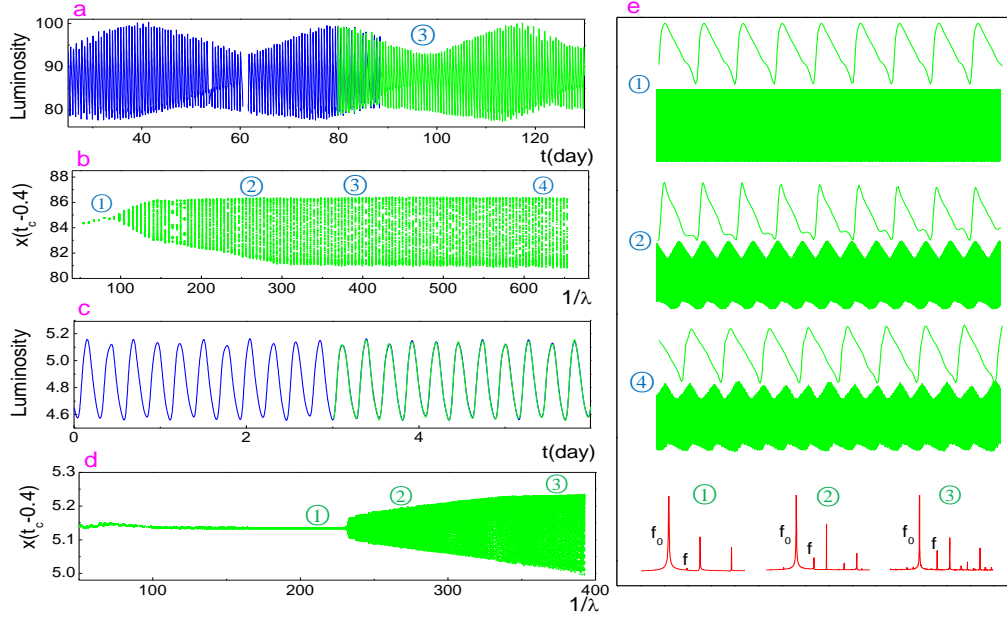


Figure 5: A prediction of variable star's evolution. (a) and (c), The blue curve is the observed light curve for KPL7198959 and KPL5520878, respectively, and the green curve is the corresponding prediction by the learning machine. (b) and (d), The bifurcation diagram of the learning machine trained by the observed light curve shown in (a) and (c), respectively. At the position marked by digit 3 in (b) and 2 in (d) the present light curves of the target stars can be best mimicked, as the green curve in (a) and in (c) shows. In (a), the prediction is accurate for subsequent five days in amplitude and keeps accurate all the time in phase. In (c), the prediction keeps accurate all the time in both the amplitude and phase. The green patterns in (e) are the predicted representative pulsation patterns of 300 days, and the green curves show a 3-day's segments, along the bifurcation diagram (at the positions marked by digits 5 in (b)). The pattern marked by digit 1 represents a stage of pure single cycle, by digit 2 a Blazhko-effect stage without period-doubling characteristics, by digit 3 a Blazhko-effect pulsation with period-doubling characteristics; The period-doubling characteristic emerges intermittently (around the left-hand side corner in (a)) as in the case of sample (around the right-hand side corner in (a)), by digit 4 it represents an irregularly modulated Blazhko-effect stage; The period-doubling characteristic can still be seen in this stage. (e) also shows the power spectra of light curves with positions marked in (d) (red curves). The amplitude of the fundamental frequency f_0 is truncated so that the gold frequency peak f is revealed. These plots indicate that the gold frequency has been appeared in the small-amplitude-change stage.

These predictions cannot be verified by direct observation. However, one can find from the Kepler database that at each predicted stage, there are a large number of qualitatively similar variable stars, which indirectly suggests that the evolution route predicted based on the bifurcation diagram may be true.

The bifurcation diagram of KPL5520878 (Fig. 5(d)) implies that it belongs to another class of variable stars with a simple evolution dynamics. The learning machine can accurately predict its light curve for all the investigated time, indicating that its pulsation is not chaotic. Meanwhile, the evolution has experienced only two stages, i.e.,

from a quasi-periodic stage at which the amplitude of the pulsation varies slightly to the next quasi-periodic stage at which it varies distinctly. We have checked that there is no Blazhko effect at both stages; the patterns marked by green digits 1, 2 and 3 look like the pattern marked by green digit 1 in Fig.5(e). During the evolution process, the fundamental frequency remains approximately the same, and another so-called golden ratio second pulsation mode, i.e., the ratio of its frequency f to the fundamental frequency f_0 is close to the golden ratio ($f_0 / f \sim 0.63$ in Fig. 5(e)), coexists as well. Other Golden stars also show the similar bifurcation diagrams (see SM-Fig. 6). Therefore, these gold stars do should belong to the same class.

Discussion

The new function of learning machine we find in this paper opens up a model-free approach to understand the global dynamics of a black-box system. This function is different from the conventional model-free approach for predicting the variable evolution using the history time series. In that scenario, the dynamical characteristics have been encoded in the history time series. What one wants to do is to predict the subsequent evolution of variables in chaotic parameter set (the application to periodic motion is trivial since it can be predicted based on the history record), but those approaches cannot infer the dynamical behavior at other parameter sets. In contrast, our approach emphasizes the application for probing the global dynamical behavior of a black-box system in a nearby parameter region using also the history time series recorded at the present parameter set, though by our method we can predict the consequent evolution of the time series at the present parameter set as well. By our approach, the primary types of the dynamical behavior of the target system can be unveiled. As our examples show, by using only a segmental time series of a limit cycle, one can infer that the target system has complex dynamical behavior from simple limit cycle to chaotic motion. Our approach thus provides a global understanding of the system dynamics.

This framework indeed provides a different idea for the inverse problem approach. Note that the learning machine approach has been widely applied to many inverse problems (21-24). Nevertheless, the motivation of those works is to determine the parameters of the model of the target system itself, following the orthodox approach of the inverse problem. The new idea here is inspired by the comprehension of following results. It has been proved that an inverse problem may have multiple solutions (1) and the multiple solutions are ubiquitous in higher dimensional systems (2), which means that different dynamical systems can produce the same output time series. Based on these observations, it is reasonable to assume that there are multiple systems whose dynamics are equivalent to or approximately equivalent to a specific target system. Therefore, instead of finding the exact equation of motion of the target system, one can train a learning machine to collapse to one of the equivalent systems, and observe the dynamical behavior of the learning machine emerged in different training stage. Though the application range as well as in what a parameter region and in what an accuracy the dynamics can be reproduced needs further studies, this

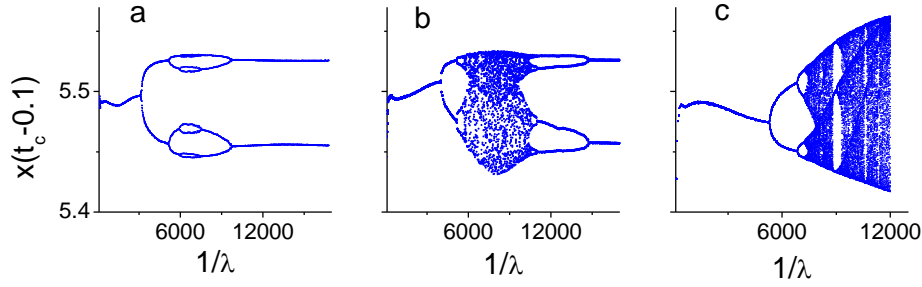
framework paves the way to understand the overall dynamical behavior of dynamical systems based on only the data of state variables at a given parameter set.

This task may be fulfilled by using other learning machines. Indeed, our learning machine can be considered as a simplified version of the reservoir computer (8-10). The essential difference is that we train the learning machine using the Monte Carlo scheme. This scheme can adjust all of the parameters of the learning machine and, particularly, can guarantee the monotonic decrease of the cost. On the contrary, the design of the reservoir computing is achieved by one step of calculation, and involves no training process. If one adopts a proper reservoir computer or other recurrence learning machines, the similar phenomenon may also be expected in the training process.

1. Giraud, O. & Thas, T. Hearing shapes of drums – mathematical and physical aspects of isospectrality, *Reviews of Modern Physics* **82** (3), 2213-2255(2010).
2. John, M. Eigenvalues of the Laplace operator on certain manifolds, *PNAS* **51** (4), 542(1964).
3. Takens, F. Detecting strange attractors in turbulence. *Dynamical Systems and Turbulence, Warwick 1980*, eds Rand, D.A. & Young, L.S. (Springer, Berlin).
4. Ma, H.F. *et al.* Randomly distributed embedding making short-term high-dimensional data predictable. *PNAS* **115**, E9994-E1002 (2018).
5. Farmer, J.D. & Sidorowich, J.J. Predicting chaotic time series. *Phys Rev Lett* **59**, 845-848 (1987).
6. Hinton, G.E., Osindero, S. & Teh, Y.W. A fast learning algorithm for deep belief nets. *Neural Comput* **18**, 1527-1554 (2006).
7. Hochreiter, S. & Schmidhuber, J. Long short-term memory. *Neural Comput* **9**, 1735-1780 (1997).
8. Maass, W., Natschläger, T. & Markram, H. Real-time computing without stable states: A new framework for neural computation based on perturbations. *Neural Comput* **14**, 2531–2560(2002).
9. Jaeger, H. & Haas, H. Harnessing nonlinearity: Predicting chaotic systems and saving energy in wireless communication. *Science* **304**, 78-80(2004).
10. Pathak, J., Hunt, B., Girvan, M., Lu, Z. & Ott, E. Model-free prediction of large spatiotemporally chaotic systems from data: A reservoir computing approach. *Phys Rev Lett* **120**, 024102(2018).
11. Lindner, J. F. *et al.* Strange nonchaotic stars. *Phys. Rev. Lett.* **114**, 0541011-0541012 (2015).
12. Benko, J. M. & Szabó R. The Blazhko effect and additional excited modes in RR Lyrae stars, *The Astrophysical Journal Letters* **809**, 1-5(2015).
13. McNamara, B. J., Jackiewicz, J. & McKeever, J. The classification of Kepler B-star variables. *The Astronomical Journal* **143**:101(2012) .
14. Benko, J. M., *et. al.* Long-timescale behavior of the Blazhko effect from rectified Kepler Data. *Astrophysical Journal Supplement* **213**, 31(2014)

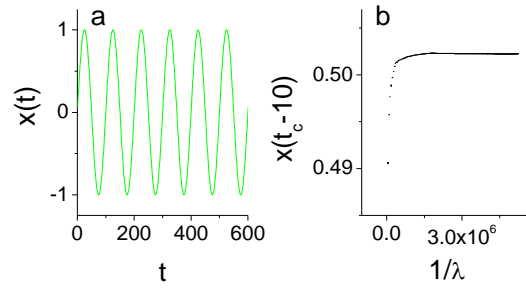
15. Szabó, R. et. al., Does *Kepler* unveil the mystery of the Blazhko effect? First detection of period doubling in *Kepler* Blazhko RR Lyrae stars. *Mon. Not. R. Astron. Soc.* **409**, 1244–1252 (2010)
16. Borucki, W. J. et al., Planet-detection mission: Introduction and first results. *Science* **327**, 977 (2010).
17. Finkbeiner, A. Astronomy: Planets in chaos, *Nature* (London) **511**, 22 (2014).
18. Jenkins, J. M. et al., Overview of the Kepler science processing pipeline, *Astrophys. J. Lett.* **713**, L87 (2010).
19. Kolenberg, K. et. al. First Kepler results on RR Lyrae stars. *The Astrophysical Journal Letters* **713**, L198–L203(2010)
20. <http://archive.stsci.edu/kepler/>
21. Poggio, T., Rifkin, R., Mukherjee, S. & Niyogi, P. General conditions for predictivity in learning theory. *Nature* **428**, 419-422(2004)
22. Tarantola, A. Popper, Bayes and the inverse problem, *Nature Physics* **2**, 492–494(2003)
23. Karianne J. Bergen, Paul A. Johnson, Maarten V. de Hoop, Gregory C. Beroza, Machine learning for data-driven discovery in solid Earth geoscience, *Science* **363**, 1299 (2019)
24. Pilozzi, L., Farrelly, F. A., Marcucci, G. & Conti, C. Machine learning inverse problem for topological photonics. *Communications Physics* **1**, 57(2018)

Supplementary Materials

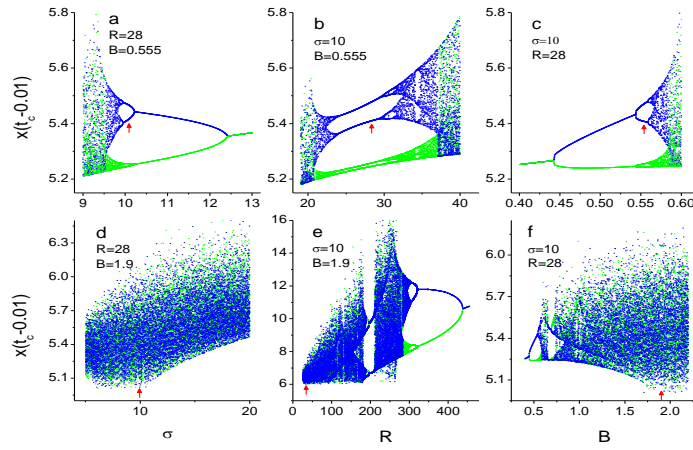


SM-Figure 1 | Finding the optimal training control parameters. The three plots are bifurcation diagrams of learning machines caused by the same training sample at $(\sigma, R, B) = (10, 28, 0.555)$. The parameter $c_\beta = 1, 0.8, 0.6$ are applied for (a), (b), and (c) respectively and with all of other training control parameters keeping fixed ($c_u = 0.2, c_v = 2, c_b = 15, M = 50, N = 3000$). We see that the last one do fully recover the dynamics of the target system, and thus this parameter together with other fixed parameters are considered to be the optimal training control parameters for this training set. While we see that the first two also achieve the partially recovery.

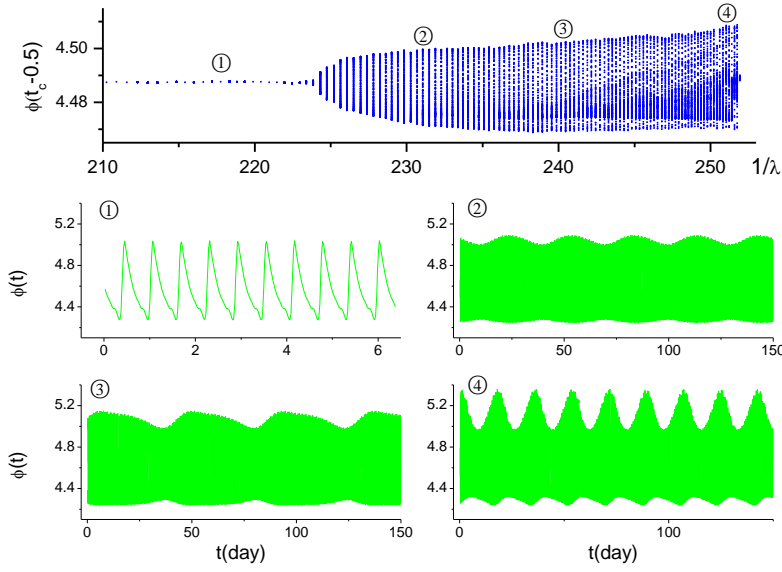
SM-Figure 2 | Every training sample made in the interval $B \in (0.45, B_c)$ leads to a similar bifurcation diagram of the target system in such an interval, i.e., Fig. 1(b) in the text. The value of parameter B is given in the corresponding plot (the first three are located in periodic windows and the last one is in the chaotic region). The other two parameters are fixed at $(\sigma; R) = (10; 28)$. In (a), (b), and (d), the output of the learning machine diverges directly at the critical point. In (c), the output bursts suddenly with trajectories losing the topological similarity to those of target system.



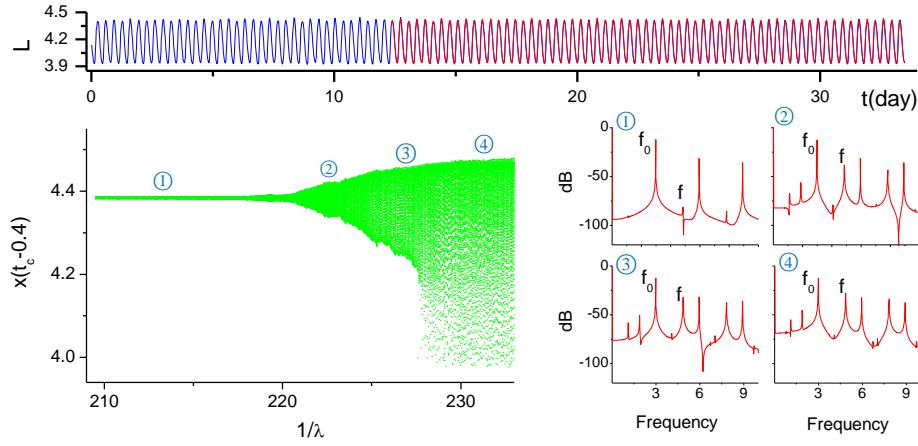
SM-Figure 3 | The training sample of a harmonic rotator (a) and the resulted bifurcation diagram of the learning machine (b). It can be seen that the learning machine remains on the present state always after a short transient period.



SM-Figure 4 | The bifurcation diagrams of the Lorenz model along different parameter axis. The arrow in the first/second line indicates the position that the first/second sample applied in Fig. 1-3 is made. Blue and green colors represent coexisting attractor branches of different symmetry, for (x,y) and $(-x,-y)$, respectively.



SM-Figure 5 |The bifurcation diagram of the learning machine trained by **KPL5559631**, another Blazhko-effect star without the period doubling characteristic. The pattern marked by digit 2 mimics the present light curve. The predicted subsequent patterns, marked by digit 3 and 4, show no period doubling bifurcation characteristic.



SM-Figure 6 | The bifurcation diagram of the learning machine trained by another Gold star **KPL4064484**. (a) The blue curve is the sample light curve and the green one is the predicted light curve. It can be seen that the prediction is almost exact. (b) The bifurcation diagram shows that this star should also experience a quasi-period stage with slight change and a quasi-period stage with remarkable change in the pulsation amplitude. (c)The power spectra of the predicted light curves indicate that the Gold frequency may become dominant gradually, though we have not seen this frequency in the first stage.